Structural Engineering and Mechanics, Vol. 38, No. 5 (2011) 593-618
DOI: http://dx.doi.org/10.12989/sem.2011.38.5.593

Analytic solution for the interaction between a viscoelastic Bernoulli-Navier beam and a winkler medium

Claudio Floris* and Francesco Paolo Lamacchia[a]

Department of Structural Engineering, Politecnico di Milano, I-20133 Milano, Italy

(Received March 29, 2010, Accepted January 15, 2011)

Abstract. This paper deals with the problem of the determination of the response of a viscoelastic Bernoulli-Navier beam, which is resting on an elastic medium. Assuming uniaxial bending, the displacement of the beam axis is governed by an integro-differential equation. The compatibility of the displacements between the beam and the elastic medium is imposed through an integral equation. In general and in particular in the case of a Boussinesq medium, the solution has to be pursued numerically. On the contrary, in the case of a Winkler's medium the compatibility equation becomes a linear finite relationship, which allows finding an original analytical solution of the problem for both hereditary and aging behavior of the beam. Some numerical examples complete the paper, in which a comparison is made between the hereditary and the aging model for the creep of the beam.

Keywords: beams; creep; analytical solution; contact problem; Winkler's elastic medium.

1. Introduction

In structural mechanics, problems of coupling materials or elements with different behaviors are frequently encountered, and such problems constitute a wide class: a bridge girder made from a reinforced concrete slab and a T-shaped steel beams; a reinforced concrete or steel beam whose supports are made from a polymeric material; a brick wall repaired by fibers of steel or of another material; a reinforced concrete column encased by a steel jacket; a beam having a continuum contact with a medium, and so on. The last problem will be analyzed in this paper.

The response of beams and plates resting on an elastic medium has been studied since the fifties. Different models were considered such as Bernoulli-Navier and Timoshenko beams, Boussinesq's, Winkler's, Kerr's, and Pasternak's media for both static and dynamic responses. Static analyses were presented by Freudenthal and Lorsh (1957), Reissner (1958), Raymondi (1959), Lee and Radok (1960), Pister and Williams (1960), Kuczma and Świtka (1990), Kuczma and Demkovicz (1992), Morfidis and Avramidis (2002), Nobili and Tarantino (2005), and by Avramidis and Morfidis (2006). Dynamic analyses were performed by Sun (2001, 2007), Elfesoufy and Azrar (2005), Kargarnovin *et al*. (2005), Kim and Cho (2006), Muscolino and Palmeri (2007), Lancioni

*Corresponding author, Associate Professor, E-mail: floris@stru.polimi.it
[a]Ph.D., Professional Engineer, Formerly Graduate Student

and Lenci (2010), and by Morfidis (2010).

The majority of the authors considered purely elastic beams and plates resting on a viscoelastic medium with a bilateral contact: among the above cited authors only Lee and Radok (1960), Kuczma and Demkovicz (1992), Nobili and Tarantino (2005) analyzed viscoelastic beams and plates. Unilateral contact was assumed by Kuczma and Świtka (1990), Kuczma and Demkovicz (1992), Nobili and Tarantino (2005), Lancioni and Lenci (2010).

In the above cited references, the coupling problem is cast according to the structural mechanics laws obtaining an analytical formulation. However, a few authors only find an analytical solution in closed form. Often, the solution is numeric, and is obtained by discretizing the equations that govern the problem. In some analyses such those by Morfidis and Avramidis (2002), Lancioni and Lenci (2010), and by Morfidis (2010) resort is made to the finite element method. *Ad hoc* beam elements are constructed: while Lancioni and Lenci consider Euler-Bernoulli beams, Morfidis and Avramidis (2002) and Morfidis (2010) consider Timoshenko beams. The models used for the beam or the plate, the medium, and the type of contact determine whether the solution is analytic or numeric. In general, to have an analytic solution, the problem must be formulated or reconducted to a differential form, and the constraint must be bilateral; otherwise, the solution is numeric.

A numeric solution for viscoelastic beams resting on Winkler's type media was obtained by Nobili and Tarantino (2005). They address the problem of the frictionless unilateral contact of an aging visco-elastic Bernoulli beam with a viscoelastic soil; a compatibility inequality is formulated, which gives raise to a numerical approach of solution: a finite difference method along the beam axis and a step by step quadrature integration in time are used. The results are in terms of displacements and contact pressures.

Lee and Radok (1960) analyze the general case of two viscoelastic bodies in contact as the counterpart of the Hertz problem in elasticity; the solution is obtained from the corresponding purely elastic solution. Kuczma and Świtka (1990) study the interaction between an elastic beam and a Winkler-type viscoelastic foundation with unilateral constraint. The problem is formulated by means of a variational inequality, and the solution is obtained by applying the finite element method. Kuczma and Demkowicz (1992) generalize the previous work to the plates giving an adaptive algorithm of solution that takes the viscosity of the beam and of the plate into account.

Reissner (1958) and Raymondi (1959) formulate the problem of the interaction in differential form, the former for a plate on a viscoelastic medium, the latter for a Bernoulli beam on a Boussinesq's medium; both do not solve the differential equations governing the respective problems. Other authors succeed in solving the governing equations, so attaining analytical solutions. Freudenthal and Lorsch (1957) analyze an infinite elastic beam resting on a viscoelastic foundation, for which the mechanical models of Kelvin, Maxwell, and Kelvin-Voigt are considered. In any case the problem is cast in differential form so that analytic solutions are found. Kargarnovin *et al*. too (2005) consider the response of infinite beams; these are supported by non linear viscous foundations and are subjected to harmonic moving loads. The dynamic analysis is developed in the frequency domain. Attention is mainly focused on the different responses of Bernoulli and Timoshenko beams, while the evolution in time of the response quantities such as bending moment and displacement is not addressed. Pister and Williams (1960) obtain an analytical solution for a thin (Lagrange-Kirchhoff) plate resting on a viscoelastic foundation by means of the Laplace transform method.

Sun analyses the dynamic responses of a Bernoulli beam (2001) and of a Kirchhoff's plate (2007) resting on a viscoelastic foundation. In the first study the viscoelasticity is described by the

Newton's model, while in the second one by Kelvin's model, and the solution is pursued by means of Fourier transform and complex analysis, which yields an analytical solution.

Elfesoufi and Azrar (2005) make a unified treatise of the buckling, flutter and vibration of a Bernoulli beam resting on an elastic foundation by using an integral formulation disregarding the creep of both the beam and the foundation. Even Avramidis and Morfidis (2006) and Kim and Cho (2006) do not consider the creep explicitly in a static and a dynamic analysis, respectively, of a beam resting on a two or three-parameter soil (Kerr 1964, 1985, Pasternak 1954).

Muscolino and Palmeri (2007) determine the dynamic response of beams resting on viscoelastically damped foundations acted by moving loads. They use a refined state space formulation having the vehicle-track interaction in mind. The method is very attractive but may be computationally heavy.

This paper addresses the problem of the interaction between a viscoelastic Bernoulli-Navier beam and an elastic medium assuming that the contact is bilateral. An analytical solution is pursued, which is surely more feasible than a numeric one, and more valuable for engineering analyses. Thus, attention is focused on beam creep. In fact, many engineering materials exhibit constitutive laws dependent on time, that is they have a viscous behavior. Among viscous materials there is concrete, from which most foundation structures are made. Creep strongly influences the response of concrete structures (Creus 1985, Bažant 1988) causing relevant differences with respect to a purely elastic response. A notable case is that of a structure in which viscoelastics members are coupled with elastic ones such as a concrete beam supported by steel columns: analytical solutions were obtained for the redundant forces (Mola 1982). The present problem can be seen as that of a structure with infinite redundant forces since the elastic constraint is distributed, and in every point a force is exchanged. The constraint is assumed to be bilateral for some reasons: (1) as advanced, an analytical solution is pursued; (2) the actual foundation beams are generally designed in such a way to avoid detachments.

After the Introduction the equilibrium equation for a beam resting on a medium is established. In the following section the compatibility between the medium and the beam is imposed with reference to both Boussinesq's and Winkler's media, then the analysis is restricted to the latter. The fourth section treats the solution of the equibrium equation for a Winkler's medium. The fifth section presents the analyses, after which there are the conclusions, the Appendix, and the references. For reader's convenience, the fundamental laws of the linear viscosity are recalled in the Appendix.

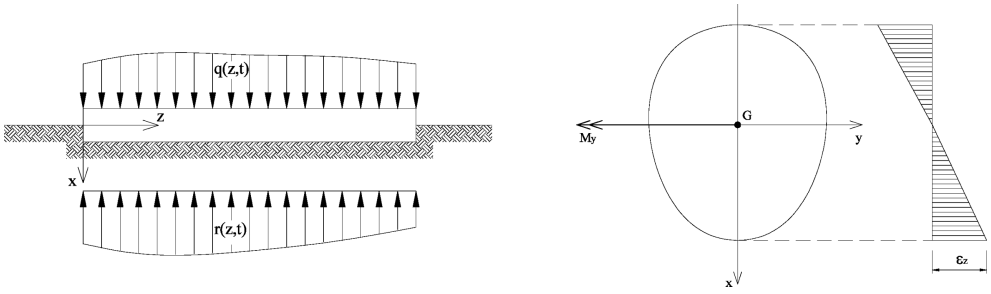

Fig. 1 Beam on an elastic medium (left), and its cross section (right)

2. Equilibrium of a viscoelastic Bernoulli-Navier beam

The theory of the Bernoulli-Navier beam is based on the hypothesis of plane section (Fig. 1, right), that is after the deformation caused by bending moment and shear force the cross-section remains plane. Basing on this hypothesis, the normal stress on the section is (the Cartesian axes are depicted in Fig. 1)

$$\sigma_z(x,z,t) = \frac{M_y(z,t)x}{I_{yy}} \tag{1}$$

where both σ_z and M_y vary with time for the twofold reason that the load q (Fig. 1) varies with time, and there is a viscous behavior (recalls on the linear theory of the viscosity are in the Appendix).

Using Eq. (1) in the superposition integral that expresses the viscous strains (Eq. (61)), we have

$$\varepsilon_z(x,z,t) = \sigma_z(t_0)J(t,t_0) + \int_{t_0}^{t} J(t,t')\frac{d\sigma_z(t')}{dt'}dt' = \frac{M_y(z,t_0)x}{I_{yy}}J(t,t_0) + \int_{t_0}^{t}\frac{\partial M_y(z,t')}{\partial t'}\cdot\frac{x}{I_{yy}}\cdot J(t,t')dt' \tag{2}$$

where t_0 denotes the instant in which the loading history begins. The instant t_0 is in general different from the instant in which beam construction is completed (for concrete the latter instant is that of complete hardening of the cementitious mixture). However, it is recalled that in the notation used for the aging model t_0 is the first instant in which the material can be loaded.

As a consequence of plane section law the beam curvature is given by

$$\frac{1}{\rho(z,t)} \cong \frac{\partial^2 v(z,t)}{\partial z^2} = -\frac{\varepsilon_z(x,z,t)}{x} \tag{3}$$

where $v(z, t)$ denotes the displacement of the beam axis in x direction. By using Eq. (3) in (2), we have

$$\frac{\partial^2 v(z,t)}{\partial z^2} = -\frac{M_y(z,t_0)}{I_{yy}}J(t,t_0) - \frac{1}{I_{yy}}\cdot\int_{t_0}^{t}\frac{\partial M_y(z,t')}{\partial t'}\cdot J(t,t')dt' \tag{4}$$

Now, we take the derivative of Eq. (4) twice keeping into account that $dM_y/dz = V_x$ (V_x is the shearing force), and $dV_x/dz = -q_x(z)$

$$\frac{\partial^2 v(z,t)}{\partial z^4} = \frac{q(z,t)}{I_{yy}}J(t,t_0) + \frac{1}{I_{yy}}\cdot\int_{t_0}^{t}\frac{\partial q(z,t')}{\partial t'}\cdot J(t,t')dt' \tag{5}$$

The load q on a beam having a continuous contact on a medium whichever is given by the difference between the external load q_x and the medium distributed reactive force r, that is

$$q(z,t) = q_x(z,t) - r(z,t) \tag{6}$$

Thus, Eq. (5) takes the first final form

$$\frac{\partial^4 v}{\partial z^4} = \frac{q_x(z,t_0) - r(z,t_0)}{I_{yy}}J(t,t_0) + \frac{1}{I_{yy}}\int_{t_0}^{t}\frac{\partial}{\partial t'}[q_x(z,t') - r(z,t')]J(t,t')dt' \tag{7}$$

Accordingly with the assumption of Poisson ratio constant in time, the elastic modulus E is constant

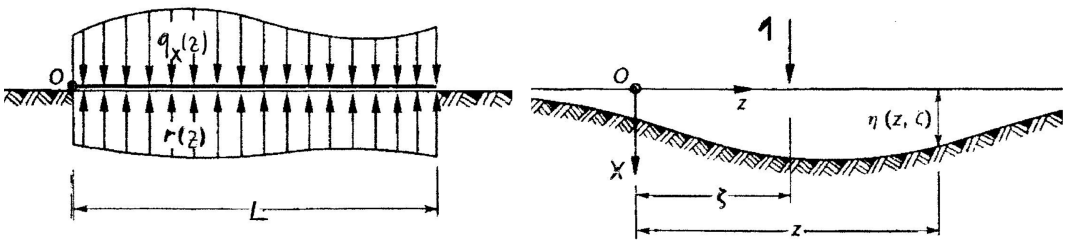

Fig. 2 Loads on the beam resting on elastic medium (left), influence function (right)

too. Recalling that $J(t,t) = 1/E$ and $L(t,t') = -E\frac{\partial J(t,t')}{\partial t'}$ being L the viscous kernel, integration by parts of Eq. (7) leads to the second form of the equilibrium equation of the beam

$$\frac{\partial^4 v}{\partial z^4} = \frac{q_x(z,t) - r(z,t)}{EI_{yy}} + \frac{1}{EI_{yy}}\int_{t_0}^{t} [q_x(z,t') - r(z,t')]L(t,t')dt' \tag{8}$$

Eqs. (7), (8) are linear integro-differential equations, whose solutions can be obtained once the reactive force r is established. This must be such that the compatibility between the displacements of the beam axis (v) and of the upper surface of the continuous medium (η) is preserved: see next section.

3. Compatibility equation

A beam having a continuum contact with a medium can be considered infinitely redundant, being the redundant forces the reactive forces $r(z)$ that the medium exerts in every contact point; the contact points constitute an infinite set (Fig. 2). To determine the redundant forces, compatibility must be imposed between the beam and the medium. In other words, the beam deflection $v(z, t)$ equates the medium vertical displacement $\eta(z, t)$. In order to express the previous equality, the mechanical properties of the medium are necessary. Several models are used in literature to idealize the soils and the other media on which a beam may lay: in this paper attention is restricted on linear media such as Boussinesq's and Winkler's ones (Boussinesq 1878, Flamant 1892, Winkler 1867, Timoshenko 1970).

For linear media the compatibility of the beam axis and the superior surface of the medium requires that the following integral equation is satisfied

$$r(z,t_0)J^*(z,t,t_0) + \int_{t_0}^{t} \frac{\partial}{\partial t'} r(z,t')J^*(z,t,t')dt' = v(z,t) \tag{9}$$

In Eq. (9) the function $J^*(z,t,t')$ gives the surface displacement of the medium to a constant unit pressure applied in t', and includes the viscous properties of the medium.

If the medium has no viscous deformation, Eq. (9) is replaced by

$$v(z) = \int_0^L \eta(z,\zeta)r(\zeta)dz \tag{10}$$

where L is beam length, and η the Green function or influence function of the medium, while the

other quantities are defined in Fig. 2. The function $\eta(z, \zeta)$ assumes different expressions according to the specific model adopted for the medium. For a Winkler's medium $\eta(z, \zeta) = k\delta(z)$ being $\delta(z)$ Dirac's delta.

A Boussinesq's medium is an isotropic and homogeneous elastic half space. Boussinesq himself and Flamant found the stress and strain distributions as well as the displacement fields for both the cases of point load and load uniformly distributed on an area A. In the case of point load the Green's function to be inserted in (10) is

$$\eta(z, \zeta) = \frac{1}{\pi|z-\zeta|}\frac{1-\nu_s^2}{E_s} \tag{11}$$

where E_s and ν_s are the elastic constants of the medium, while z and ζ are the abscissae of two points on a line, which in this case is the beam axis. The shortcoming of Eq. (11) is that it diverges when $z \to \zeta$: to avoid this, when $z \approx \zeta$ Eq. (11) must be replaced by the Green's function for the case of a uniformly distributed load q on a rectangular area

$$\eta(z) = qI_\eta b_1 \frac{1-\nu_s^2}{E_s} \tag{12}$$

where b_1 is the smaller side of the rectangle, the point of abscissa z is the centroid of the rectangle, while I_η is a numerical coefficient depending on the ratio b_1/b_2 (see Timoshenko 1970, Bowles 1982). The necessity of varying the influence function renders the evaluation of the integral (10) more cumbersome.

Thus, in the case of a Boussinesq medium the problem is governed by Eqs. (8), (10). Raymondi (1958) showed that the problem can be reduced to a differential form. When the beam has viscous strains, the solution can be found numerically: a specific algorithm has been developed by the writers, and it is not reported here. In the following reference will be made to Winkler's medium.

4. Solution of the equilibrium equation

4.1 Winkler's medium, restrained beam

In order to derive the analytic solution of the integro-differential Eq. (8), the cases of beam with restrained ends and of free ends must be treated separately. A restrained beam is depicted in Fig. 3.

Inserting the influence function of a Winkler's medium into Eq. (10), it is obtained

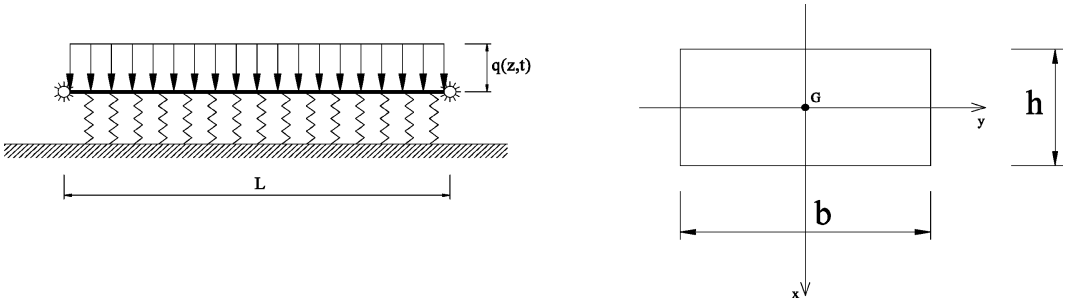

Fig. 3 Hinged-hinged beam on Winkler's medium and its cross section

$$r(z,t) = kv(z,t) \tag{13}$$

After substituting Eq. (13) in (8), this changes into

$$\frac{\partial^4 v(z,t)}{\partial z^4} + \eta^4 v(z,t) + \eta^4 \int_{t_0}^{t} v(z,t')L(t,t')dt' = \overline{q}_x(z,t) + \int_{t_0}^{t} \overline{q}_x(z,t')L(t,t')dt' \tag{14}$$

where $\eta^4 = \frac{k}{EI_{yy}}$, $\overline{q}_x = \frac{q_x}{EI_{yy}}$

Separating the variables, a series solution is expressed as

$$v(z,t) = \sum_{k=1\ldots\infty} {}_k\phi_k(z)V_k(t) \tag{15}$$

The functions $\phi_k(z)$ must satisfy the boundary conditions, and constitute a complete orthonormal basis in $\mathcal{L}^2$. If the ϕ_k's are such, the following properties hold

$$\int_{t_0}^{t} \phi_j(z)\phi_k(z)dz = \delta_{jk} \tag{16}$$

$$\frac{d^4\phi_k(z)}{dz^4} = \lambda_k^4\phi_k(z) \tag{17}$$

where δ_{jk} is Kronecker's delta, and λ_k are the eigenvalues. The eigenfunctions of the free vibrations of the same beam enjoy this properties. Thus, the required ϕ_k's are obtainable by solving the free vibration problem for the same beam, which is given by Clough and Penzien (1982)

$$EI_{yy}\frac{\partial^4 v}{\partial z^4} + \overline{m}\frac{\partial^2 v}{\partial t^2} = 0 \tag{18}$$

where $\overline{m}$ is the mass for unit length of the beam.

Let the sequence of the ϕ_k's available: now, Eq. (15) is substituted into (14). Multiplying both sides by $\phi_j(z)$, integrating between 0 and L, keeping Eqs. (16), (17) into account gives raise to

$$(\lambda_k^4 + \eta^4)\Phi_k V_k(t) + \eta^4\Phi_k \int_{t_0}^{t} v(z,t')L(t,t')dt' = \int_0^L \phi_k(z)\overline{q}_x(z,t)dz + \int_{t_0}^{t} [\int_0^L \phi_k(z)\overline{q}_x(z,t)dz]L(t,t')dt' \tag{19}$$

where $\Phi_k = \int_0^L \phi_k^2 dz$. The right-hand side of Eq. (19) represents the modal load, independent of z, for which we make the position

$$Q_k = \frac{\int_0^L \phi_k(z)\overline{q}_x(z,t)dz}{\Phi_k} \tag{20}$$

Inserting Eq. (20) in (19), an infinite set of Volterra's integral equations is found as

$$(\lambda_k^4 + \eta^4)V_k(t) + \eta^4 \int_{t_0}^{t} V_k(t')L(t,t')dt' = Q_k(t) + \int_{t_0}^{t} Q_k(t')L(t,t')dt' \tag{21}$$

Putting

$$\gamma_k = (\lambda_k^4 + \eta^4)^{-1} \qquad D_k = \frac{\eta^4}{\lambda_k^4 + \eta^4} \qquad \overline{D}_k = 1 - \frac{1}{D_k} \tag{22-24}$$

dividing Eq. (21) by $\lambda_k^4 + \eta^4$, this assumes the form

$$V_k(t) + D_k \int_{t_0}^{t} V_k(t')L(t,t')dt' = \gamma_k Q_k(t) + \gamma_k \int_{t_0}^{t} Q_k(t')L(t,t')dt' \quad (k = 1, 2, \ldots) \tag{25}$$

The integral Eq. (25) has the same form as the equation that gives the redundant forces of a once redundant structure made from an elastic part and a viscoelastic one (Mola 1982). If there are N redundant forces, the equations are N, while here the equations are infinite. In the analysis of a non homogeneous once redundant structure a coupling parameter D is defined as $\delta_c/(\delta_c + \delta_e)$ where δ_c is the compliance of the viscoelastic part, and δ_e that of the elastic part. For analogy, D_k is named the modal coupling parameter, and from inspection of Eq. (23) it is seen that has the same structure as that of D. Like D, D_k near one denotes a situation in which the deformability of the viscoelastic beam is prevailing, while, if D_k is small, the deformability is larger in the elastic medium.

Because of the linearity of Eq. (25), the solution is cut into two parts, that is $V_k = X_k + Y_k$. If the quantity $\gamma_k D_k Q_k - \gamma_k D_k Q_k$ is added to the right hand side of (25), this results from the sum of the following integral equations that X_k and Y_k obey to, respectively

$$X_k(t) + D_k \int_{t_0}^{t} X_k(t')L(t,t')dt' = \frac{\gamma_k}{D_k} Q_k(t) + D_k \int_{t_0}^{t} \frac{\gamma_k}{D_k} Q_k(t')L(t,t')dt' \tag{26}$$

$$Y_k(t) + D_k \int_{t_0}^{t} Y_k(t')L(t,t')dt' = \gamma_k Q_k(t) - \frac{\gamma_k}{D_k} Q_k = \gamma_k \overline{D}_k Q_k(t) \tag{27}$$

Eq. (26) is clearly satisfied by $X_k(t) = \gamma_k Q_k(t)/D_k$.

If the superposition integral (Eq. (61) of the Appendix) with $\varepsilon_n = 0$ is integrated by parts, keeping the definition (64) of the viscous kernel in mind, we obtain

$$\varepsilon(t, t_0) = \frac{\sigma(t)}{E} + \int_{t_0}^{t} \sigma(t')L(t,t')dt' \tag{28}$$

If the function $\varepsilon(t, t_0)$ is known, Eq. (28) is a Volterra's integral equation in the unknown $\sigma(t')$, whose formal solution is (see Eq. (62) of the Appendix)

$$\sigma(t) = \varepsilon(t_0)R(t, t_0) + \int_{t_0}^{t} R(t,t') \frac{\partial \varepsilon(t', t_0)}{\partial t'} \tag{29}$$

By inspection of Eq. (27), it is found that the right hand side can be interpreted as an impressed strain and Y_k as the corresponding stress, that is Eq. (27) is a particular form of the superposition integral (28), whose inverse is Eq. (29). Thus, the solution to Eq. (27) is

$$Y_k(t) = \gamma_k \overline{D}_k Q_k(t_0) R_k^*(t, t_0) + \overline{D}_k \gamma_k \int_{t_0}^{t} \frac{\partial Q_k(t')}{dt'} R_k^*(t, t')dt' \tag{30}$$

The function $R_k^*(t, t_0)$ is the so called reduced relaxation function associated with the varied viscous kernel $L_k^*(t, t_0) = D_k \cdot L(t, t_0)$ (Mola 1982). The two functions must satisfy the integral Eq. (60) of the Appendix, which in this case reads as

$$1 = \frac{R_k^*(t,t_0)}{E} + \int_{t_0}^{t} R_k^*(t,t_0)\frac{\partial J_k^*(t',t_0)}{\partial t'}dt' \tag{31}$$

Thus, to obtain the problem solution, the integral Eq. (31) must be solved before. On the other hand, that is not necessary if creep is described by both the hereditary model and the aging model.

By summing up the expressions of X_k and Y_k, the analytical solution of Eq. (25) is

$$V_k(t) = \frac{\gamma_k}{D_k}Q_k(t) + \frac{\gamma_k\overline{D}_k}{E}Q_k(t_0)R_k^*(t) + \frac{\gamma_k\overline{D}_k}{E}\int_{t_0}^{t}\frac{dQ_k(t')}{dt'}R_k^*(t')dt' \tag{32}$$

When the creep law is either hereditary or of pure aging type, the varied kernel L_k^* is simply $D_k \cdot L(t,t')$: looking at Eqs. (64), (68) of the Appendix, it is clear that the effect of multiplying by D_k is to change the parameter φ_∞ (see the Appendix at the foot of Eq. (64)). Hence, the reduced relaxation function is immediate. The couples L_k^* and R_k^* are given below for the two basic creep models

$$L_k^*(t,t_0) = D_k \cdot L(t,t_0) = D_k\alpha\varphi_\infty \cdot \exp[-\alpha(t-t_0)] \tag{33}$$

$$R_k^*(t,t_0) = \frac{E}{1+D_k\varphi_\infty}\{1 + D_k\varphi_\infty \cdot \exp[-\alpha(t-t_0)]\} \tag{34}$$

$$L_k^*(t,t') = D_k \cdot L(t') = D_k\beta\varphi_\infty \cdot \exp[-\beta(t-t_0)] \tag{35}$$

$$R_k^*(t,t') = E \cdot e^{-D_k\varphi_\infty}\{\exp[-\beta(t'-t_0)] - \exp[-\beta(t-t_0)]\} \tag{36}$$

Unfortunately, the product creep laws, such as those that are proposed by some authors and codes (Aroutiounian 1957, Bažant and Panula 1978, Bažant and Chern 1985, American Concrete Institute 1992, CEB 1984, 1993), do not enjoy this useful property: Eq. (31) has to be solved numerically, and R_k^* results in a numerical form. This is why only the hereditary and aging creep models are considered here.

If the load is constant in time, Eq. (32) reduces to

$$V_k(t) = \frac{\gamma_k}{D_k}Q_k + \frac{\gamma_k\overline{D}_k}{E}Q_kR_k^*(t) = \frac{\gamma_k}{D_k}Q_k[1-(1-D_k)\overline{R}_k^*(t,t_0)] \tag{37}$$

where $\overline{R}_k^* = R_k^*/E$. $V_k(t)$ increases with time since the second quantity in the square parentheses is decreasing due to the decreasing nature of every relaxation function. The amount of decrease is governed by the parameter D_k: as D_k tends to one, the decrease becomes negligible. Thus, keeping the previously explained meaning of this parameter in mind, viscous effects are expected to be larger for a soft elastic medium. Since this trends is common to all V_k's, the deflection $v(z, t)$ increases with time. Once $v(z, t)$ is computed, the internal forces in the beam result from the usual relations $M(z,t) = -EI_{yy}v''(z,t)$, $V_x = -EI_{yy}v'''(z,t)$. Since these relations require the second and the third derivative of a series expansion, more terms are to be retained than those strictly necessary for a good representation of $v(z,t)$.

4.2 Winkler's medium, free-end beam

Now, Eq. (14) has to be solved for the case of a beam with free ends. This scheme is common in

geotechnical engineering. The equilibrium equation is the same, but a partly different strategy is necessary as a beam with free ends has rigid motions in its plane. In fact, the eigenfunctions of the free vibrations of the same beam include the rigid motions, that is

$$\begin{aligned} \phi_0 &= a_0 \\ \phi_1 &= a_1 z \end{aligned} \tag{38}$$

where a_0 and a_1 are constant with respect to z. The other eigenfunctions have the form

$$\phi_k(z) = \mathrm{Ch}\frac{\lambda_k}{L}z + \cos\frac{\lambda_k}{L}z - \frac{\mathrm{Ch}\lambda_k - \cos\lambda_k}{\mathrm{Sh}\lambda_k - \sin\lambda_k}\cdot\left(\mathrm{Sh}\frac{\lambda_k}{L}z + \sin\frac{\lambda_k}{L}z\right) \tag{39}$$

In Eq. (39) λ_k are the eigenvalues that are obtained from solving the equation $\mathrm{Ch}\lambda_k \cdot \cos\lambda_k = 1$. The two eigenfunctions of Eq. (38) are not orthogonal to the family (39).

For that reason the solution is looked for in the form

$$v(z,t) = v_0(t) + v_1(t)\cdot z + \sum_{k=1}^{+\infty} \phi_k(z)\cdot V_k(z) \tag{40}$$

where the functions $\phi_k(z)$ are given by Eq. (39). In order to exploit the expression (40), the load must be decomposed in three parts, a uniformly distributed load, a linearly varying load, and a non linearly variable load, that is

$$q_x(z,t) = q_m(t) + q_1(t)z + q^*(z,t) \tag{41}$$

Because of the linearity of Eq. (14), the principle of superposition applies. Thus, the solutions to the three load parts of Eq. (41) are computed separately, and the global solution is obtained by summing up them. As regards the first part $q_m(t)$, which is constant along the z axis but variable in t, the displacement $v(z,t) = v_0(t)$ must be independent of z. Thus, the solution is clearly

$$v_0(t) = \frac{q_m(t)}{k} \tag{42}$$

The displacement $v_0(t)$ is independent of z so that it does not cause any internal force in the beam, and, hence, any strain; it varies in time only if q_m varies. As a consequence, creep strains cannot develop. Nevertheless, this contribution must be taken into account in the deflection line This finding is quite analogous to the case of a purely elastic Bernoulli beam on a Winkler soil subject to a uniformly distributed load q: it has a constant deflection given by $v_P(z) = q/k$ and no bending moment.

As concerns with the load $q_1 z$, substituting the second term of (40) into Eq. (14), it becomes

$$\eta^4 z\cdot v_1(t) + \eta^4 z\int_{t_0}^{t} v_1(t')L(t,t')dt' = \bar{q}_1 z + \int_{t_0}^{t} \bar{q}_1 z L(t,t')dt' \tag{43}$$

where $\bar{q}_1 = q_1/EI_{yy}$. Eq. (43) is evidently satisfied by

$$v_1(z,t) = \frac{q_1(t)}{k} \tag{44}$$

Likewise in the previous case, any internal force and creep effect do not exist. Notice that Eq. (44) is retrieved by solving the equilibrium equation of an elastic beam resting on a Winkler's

foundation subjected to a linearly varying load

By inserting $q^*(z,t)$ into Eq. (14), we have

$$v_3^{IV}(z,t) + \eta^4 v_3(z,t) + \eta^4 \int_{t_0}^{t} v_3(z,t')L(t,t')dt' = \frac{q^*(z,t)}{I_{yy}} + \frac{1}{EI_{yy}} \cdot \int_{t_0}^{t} q^*(z,t')L(t,t')dt' \tag{45}$$

in which the viscoelastic deflection due to $q^*(z,t)$ is denoted by $v_3(z,t)$, which is the only responsible of bending moment, shear and creep effects. Eq. (45) has the same form of Eq. (14): thus, one has to proceed in much the same way by using the eigenfunctions (39). The solution is given by Eq. (32). The second and the third derivative with respect to z of the displacement $v_3(z,t)$ yield the bending moment and the shear force, respectively, while, to obtain the total displacement it is necessary to add the rigid contributions, that is the first and the second term in Eq. (40).

4.3 Beam subjected to partially distributed and concentrated loads

In previous analyses the beam is loaded by a distributed force acting along the whole beam axis. On the other hand in many cases the load is distributed only on a part of the span, and in the limit it may be a concentrated force. Thus, it is necessary to extend the previous results to such loading cases.

First, let us consider a constant load q acting from the abscissa a to the abscissa $d = a + c$ (the Cartesian axes are always those shown in Fig. 1). Mathematically, the load is expressed as

$$q(z) = \begin{cases} q & a \le z \le d \\ 0 & \text{elsewhere} \end{cases} \tag{46}$$

This function is expanded in a cosine Fourier series

$$q(z) = \frac{a_0}{2} + \sum_{1}^{+\infty}{}_k a_k \cos\frac{k\pi}{L} z \tag{47}$$

where

$$a_0 = 2\frac{c}{L}q \qquad a_k = \frac{2}{k\pi} q\left(\sin\frac{k\pi d}{L} - \sin\frac{k\pi a}{L}\right) \tag{48, 49}$$

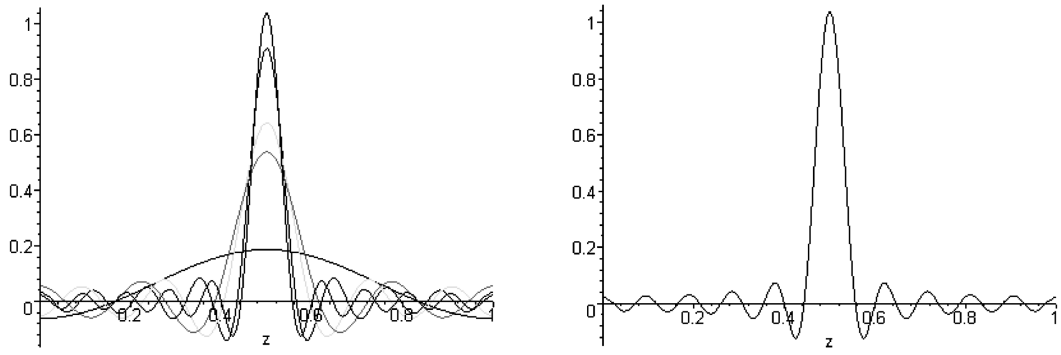

Fig. 4 Fourier series expansion of a load distributed on 1/16 of the beam span centered at midspan: left comparison among the expansions with increasing terms (blue 3 terms, green 8 terms, yellow 10 terms, violet 16 terms, red 20 terms); right twenty term expansion

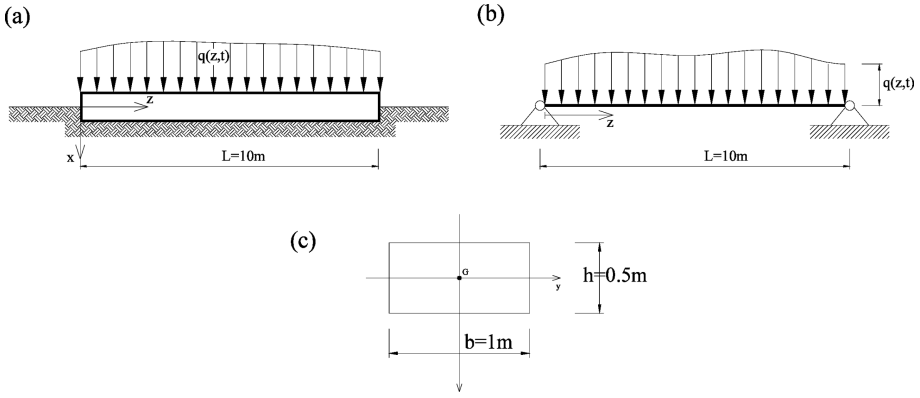

Fig. 5 (a) Unrestrained beam, (b) hinged-hinged beam, (c) beam cross section

The previous expansion is shown in Fig. 4, where both L and q are normalized to 1. It can be seen that the convergence is lengthy, and not less than 20 terms are necessary to have an acceptable matching.

A concentrated load in the abscissa $z = a$ can be mathematically described by means of Dirac's delta translated in $z = a$, that is $q(z) = P \cdot \delta(z-a)$ (Gorman 2008). Its series expansion is

$$q(z) = P \cdot \delta(z-a) = \sum_{k=1,3,5,\ldots} b_k \sin\frac{k\pi}{L} z \tag{50}$$

where

$$b_k = \frac{2P}{L} \sin\frac{k\pi a}{L} \tag{51}$$

The series (50) converges slower than the series (47), and not less than 30 terms are necessary to acceptably reproduce the spike. The series (47) can be directly used in both Eqs. (32), (45), and the term a_0 gives the constant part of the load. Viceversa, the series (50) must be subjected to the decomposition (41) before using Eq. (45).

5. Applications

The solutions obtained in previous sections for the viscoelastic analysis of a Bernoulli-Navier beam resting on a Winkler's medium have been tested considering some examples. Suitable programs have been written that perform the computations.

The beam (Fig. 5), which is made from concrete, has: L = 10 m, b = 1.00 m, h = 0.50 m, E_c = 35000 Mpa, denoting the beam length, width, height, and elastic modulus, respectively. The soil is characterized by the elastic parameters, that is the elasticity modulus E_S = 35 MPa and the Poisson ratio ν = 0.3. From E_c and ν the Winkler's constant k =18.27 MPa is obtained according soil mechanics principles (e.g., see Bowles 1982). The parameters of the creep laws (Eqs. (63)-(65), (67)-(69) of the Appendix) are: $\alpha = \beta = 0.0025$ (days)$^{-1}$, $\varphi_\infty = 3.5$, $t' = t_0 = 0$ days. In some examples the length L and the loading instant t' vary.

As regards the beam with restrained ends, these are both hinged (Fig. 5(b)) so that the eigenfunctions ϕ_k in Eq. (15) are $\sin(k\pi z/L)$ $(k = 1, 2, \ldots, N)$. The load is uniformly distributed

taking the value $q_x = 100000$ N/m; it is constant in time and is applied at time t_0, which is the instant of complete drying of the concrete.

A uniformly loaded beam on a Winkler's soil has no internal forces, and this fact has been retrieved again in previous sections. Thus, the load on the beam with free ends is variable along the span. For simplicity's sake, the loading distribution is given by the sum of a constant part, the dead load g, and a sinusoidal part in such a way the load is already decomposed according to Eq. (41) with $q_1 = 0$

$$q_x(z,t) = g + q_M \cdot \sin\left(\frac{\pi}{L}z\right) \tag{52}$$

where $g = 12262$ N/m, $q_M = 50000$ N/m.

5.1 Hinged-hinged beam with distributed load

The case of a hinged-hinged beam of length $L = 10$ meters, bearing a uniformly distributed load will be treated in this section. When the load is applied, the solution is purely elastic, and is given by the solution the classic differential equation of a beam on a Winkler's soil (Winkler 1867, Bowles 1982)

$$EI_{yy}v^4(z) + kv(z) = q_x(z) \tag{53}$$

with boundary conditions $v(0) = v(L) = v''(0) = v''(L) = 0$. The elastic displacement of the beam axis and the bending moment diagrams are in Fig. 6, where the negative signs in the graphs are caused by the plotting routine that has been used as in all the following plots.

Both the hereditary and the aging model have been used in the analyses. The plots deriving from the hereditary creep model are in Fig. 7. The deformed shape of the beam axis does not change with time, and the largest deflection has a limited increase what is probably due to the continuous restraint given by the Winkler medium. On the contrary, the bending moment changes sharply with time. At loading it is rather flat with a largest value of 170000 N·m about, and it is quite similar to the elastic solution of Fig. 6. As time passes, the central part of the span is unstressed with a marked minimum of M, while two peaks form near the supports, which at 10000 days from loading reach 300000 N·m about, that is a 90% increase with respect to the elastic solution of Fig. 6. This

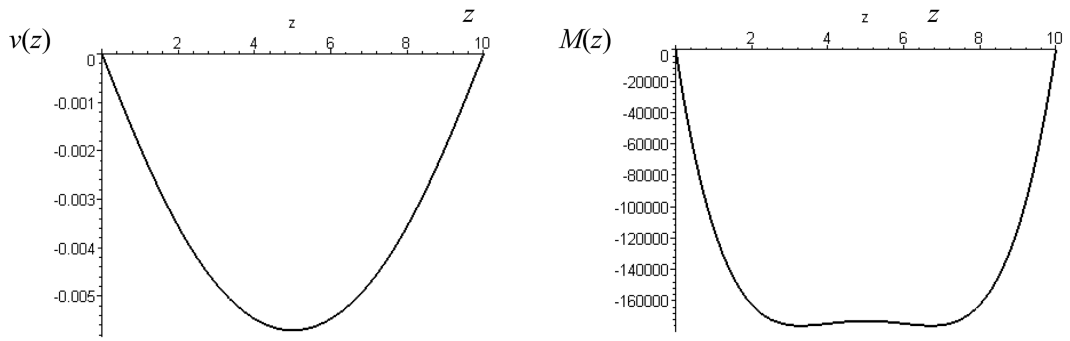

Fig. 6 Hinged-hinged beam, elastic solution: vertical displacement (m) (left) and bending moment (Nm) (right)

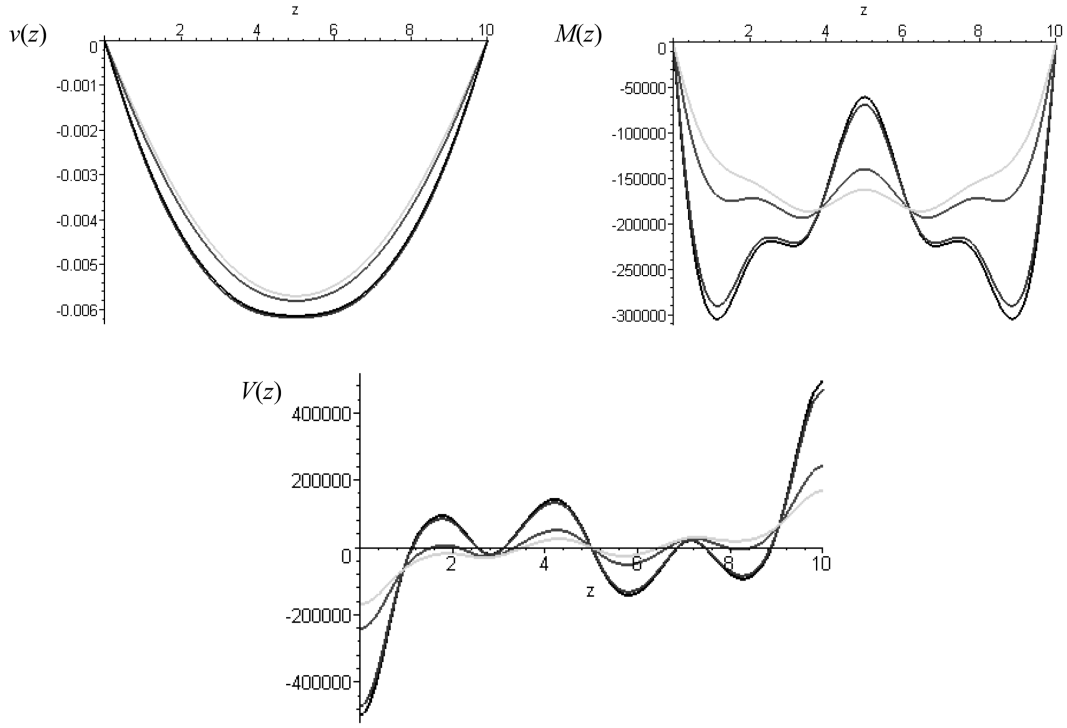

Fig. 7 Hinged-hinged beam, creep hereditary model: time evolutions of the vertical displacement (m) (top left), bending moment (N·m) (top right), shear force (bottom), loading at $t' = 0$; green line $t = 0$ days, brown 100 days, blue 1000 days, black 10000 days

finding is important inasmuch as the safety coefficient of a concrete beam is only a bit larger than 2 (≈2.25 in many cases). Two explanations are possible. First, the deflection and hence its second derivative, the bending moment, are given by the sum of sinusoidal eigenfunctions each of which represents a deformed shape of the beam. The development of the viscous deformations causes the activation of eigenfunctions of higher order that have more inflexion points. A physical explanation is that the two largest values of M near the supports are caused by the reactive forces in the hinges. The shear force increases in time in an analogous manner, but its diagram does not change shape. In general, the displacement pattern is dominated by the first viscous mode, a sinusoid, while more modes influence the bending moment and the shear force. This is due to the fact that the terms of the series giving the moment and the shear are multiplied by $(k\pi/L)^2$ and $(k\pi/L)^3$ respectively so that the weight of the successive modes is larger.

In Fig. 8 there are the diagrams obtained by using the creep aging model. As expected, they look like the corresponding diagrams of Fig. 7: in fact, the parameters and the loading time are the same. The effects of the loading time will be analyzed next.

Clearly, the presence and the type of the restraints at the beam ends influence both the displacements and the diagrams of the internal forces, but the restraint effects become lesser and lesser as the beam length increases. In order to highlight these effects, the analyses have been repeated even for $L = 5$, 20 m, holding the constant in time and space loading distribution equal to $q_x = 100000$ N/m, being the load applied in $t_0 = 0$. In Fig. 9 there are the time evolutions of the

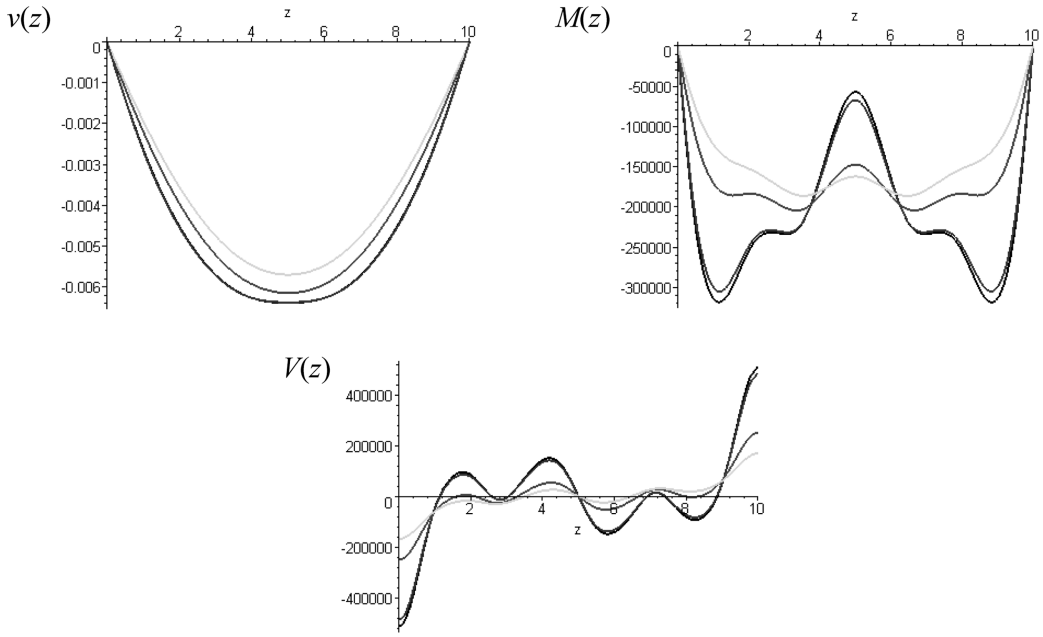

Fig. 8 Hinged-hinged beam, creep aging model: time evolutions of the vertical displacement (m) (top left), bending moment (N·m) (top right), shear force (N) (bottom), loading at $t' = 0$; green line $t = 0$ days, brown 100 days, blue 1000 days, black 10000 days

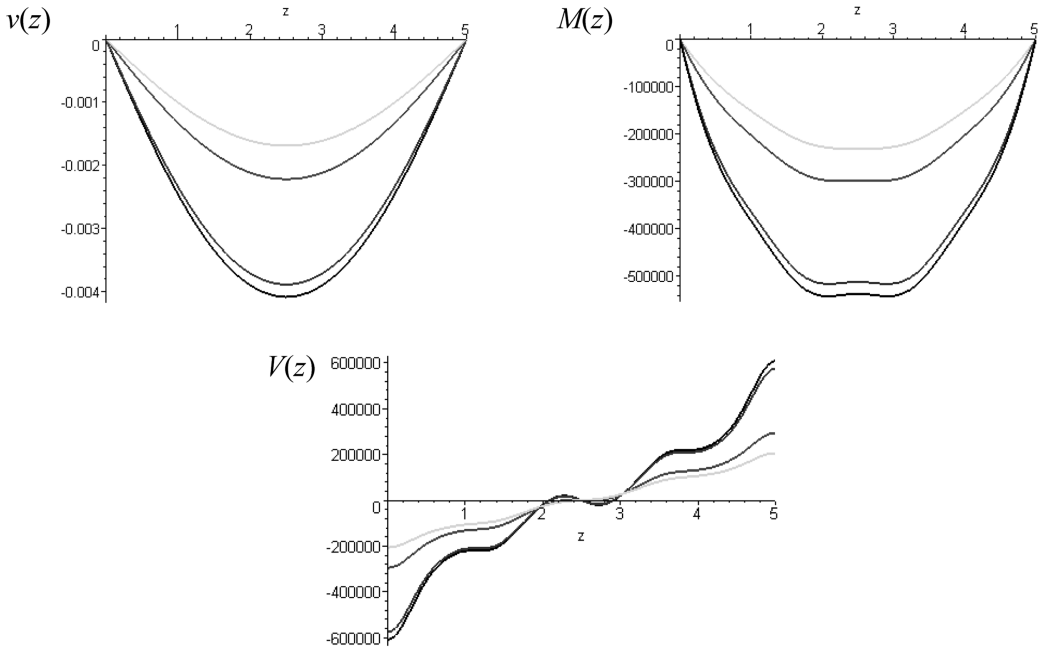

Fig. 9 Hinged-hinged beam with $L = 5$ m, creep hereditary model: time evolutions of the vertical displacement (m) (top left), of the bending moment (N·m) (top right), and of the shear force (N) (bottom), loading at $t' = 0$; green line $t = 0$ days, brown 100 days, blue 1000 days, black 10000 days

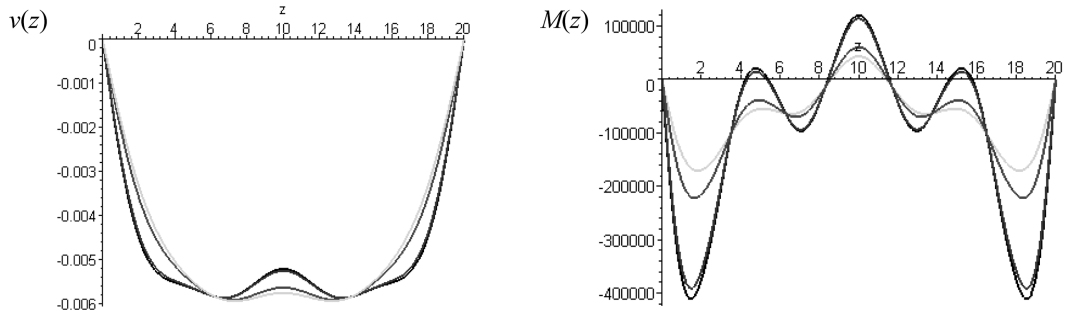

Fig. 10 Hinged-hinged beam with L = 20 m, creep hereditary model: time evolutions of the vertical displacement (m) (left), and of the bending moment (N·m) (right), loading at $t' = 0$; green line $t = 0$ days, brown 100 days, blue 1000 days, black 10000 days

viscoelastic line, the bending moment, and the shear force for L = 5. For L = 20 m the first two diagrams are reported in Fig. 10.

As regards the short beam, the increase in time of the quantities depicted in Fig. 9 is very marked: roughly, the increase is a 150% about, which is larger than that of the 10 m long beam. The shapes of the bending moment and shear force diagrams are more regular: for a short beam the higher viscous modes are less excited.

The 20 m long beam has a behavior different from those of the other two beams (Fig. 10). The deflections do not increase in time, and have a limited variation along the most part of the beam span, which resents the effect of the end restraints little. In the midspan, the displacement diminishes with time of a small amount. As regards the bending moment, it increases by a 150% in 10000 days when the asymptote of the viscous law is practically reached. There are two maxima near the supports and three minima along the span, one exactly in the midspan, as expected since the diagram must be symmetric with respect the midspan. In the vicinity of the minima the bending moment stretches the upper fibers of the beam.

When the load is applied in t_0, the first instant in which the concrete can be loaded, the analyses performed by using the aging model yield results nearly coincident with those of the hereditary creep model. The differences between the models are evident only if the load is applied in $t' > t_0$, when the material has already aged. Hereditary behavior means independence of the instant t' in which the load is applied, and in any interval Δt equal viscous strains are developed. After a given time delay the hereditary model gives the same results, independently from the instant in which the load begins. On the contrary, aging of concrete means that the farther from t_0 is t', the lesser is creep: hence there are less viscous effects. Using the aging model, the analyses have been repeated by varying the instant t' of application of the load: 100, 1000 days after the first instant t_0 in which the beam can be loaded. The diagrams are in Figs. 11, 12, respectively.

Examining the diagrams of Fig. 11, which refer to a load applied after a relatively brief time from the hardening of concrete, 100 days, notable viscous deformations are still detected, especially for the bending moment. The increase of the latter is important even if smaller than that for loading in t_0. If the beginning of loading is later (1000 days, Fig. 12), very few viscous deformations develop: they are negligible with respect to the elastic initial ones, and both the displacements and the bending moment increase of a very small quantity. This trend cannot be revealed by the hereditary creep model.

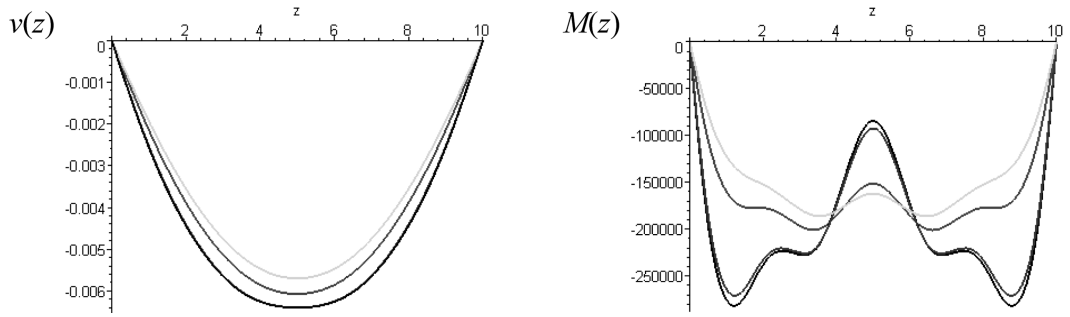

Fig. 11 Hinged-hinged beam with length L = 10 m, aging viscous model, loading in t' = 100 days: time evolutions of the displacement (m) (left), and of the bending moments (right); deflections and bending moment at loading (green), 100 days from loading (brown), 1000 days (blue), 10000 days (black)

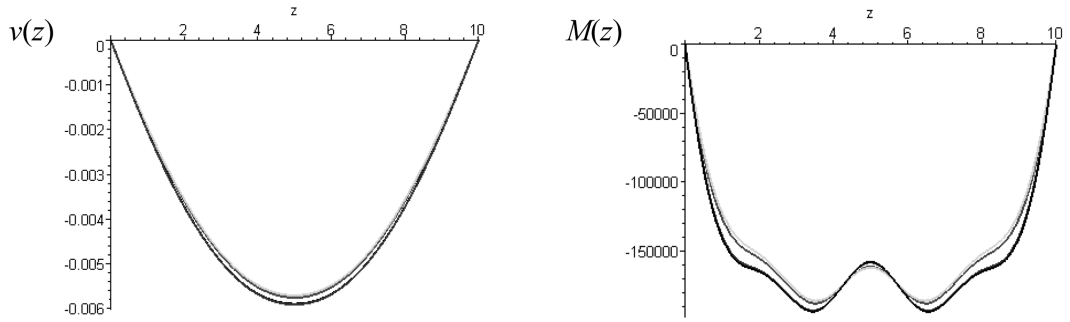

Fig. 12 Hinged-hinged beam with length $L = 10$ *m*, aging viscous model, loading in t' = 1000 days: time evolutions of the displacement (m) (left), and of the bending moments (right); deflections and bending moment at loading (green), 100 days from loading (brown), 1000 days (blue), 10000 days (black)

5.2 Free-end beam

Now, the unrestrained beam with length L = 10 m is examined. It bears its dead load and a sinusoidal loading distribution: the former load causes a rigid settlement of the beam without internal forces, and, hence, no viscous strains. Since a linearly distributed load is absent, in Eq. (40) $v_1(z,t)$ is zero. Thus, the viscoelastic deflection reduces to

$$v(z,t) = v_0(t) + \sum_{k=1}^{+\infty} \phi_k(z) \cdot V_k(t) \tag{54}$$

The rigid settlement is easily calculated, and is $v_0(t) = g/k$ = 0.0007 m, being g = 12262.5 N/m. The variable part of the displacement is obtained by solving Eq. (45) under the sinusoidal load of Eq. (52); both the hereditary and the aging viscous models are considered.

The plots deriving from the hereditary model are in Fig. 13, where there are the time evolutions of the viscoelastic displacement, of the bending moment, and of the shear force. In this case, the first eigenfunction, which is plotted in Fig. 14, is dominant on the other viscous modes as the first modal load is 36 times larger than the third modal load, being the even modal loads zero. As

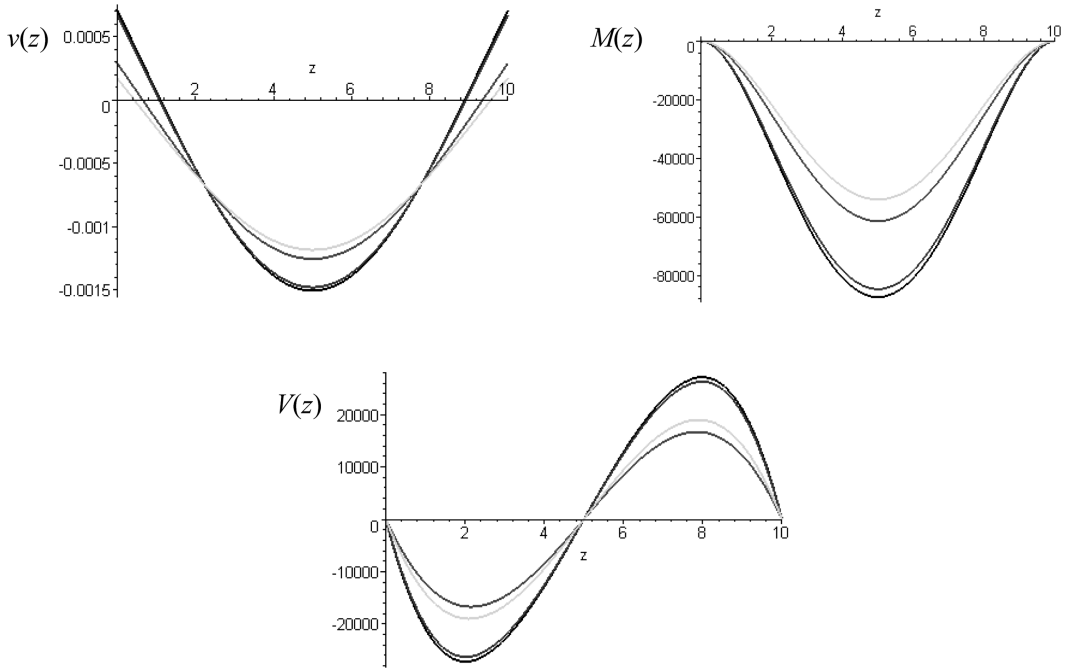

Fig. 13 Free end beam, creep hereditary model: time evolutions of the vertical displacement (m) (top left), bending moment (N·m) (top right), shear force (bottom), loading at $t' = 0$; green line $t = 0$ days, brown 100 days, blue 1000 days, black 10000 days

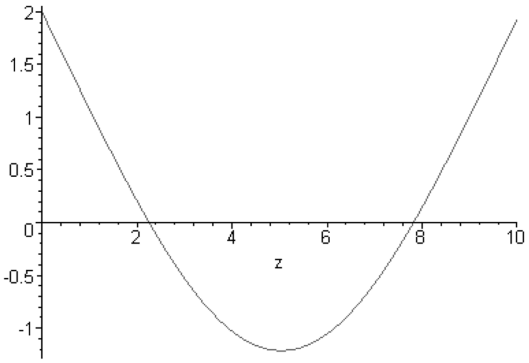

Fig. 14 First eigenfunction of the free-end beam (Eq. (56))

regards the displacements, already at the application of the load limited portions of the beam near the ends are subjected to tensile forces that can be transmitted because of the hypothesis of bilateral restraint. The development of the viscous strains amplifies the deformed line: the largest deflection increases from 0.0011 m to 0.0015 m, while the parts with tensile forces are enlarged, and the beam ends rise. Clearly, in real beams the transmission of tensile forces is not possible, but equally the lateral parts of the beam uplift, which must be avoided in engineering practice.

The bending moment (right plot of Fig. 13) has a more marked increase in time, from 50000 N·m to 90000 N·m about 10000 days after the loading. The moment diagrams are bell-shaped in any

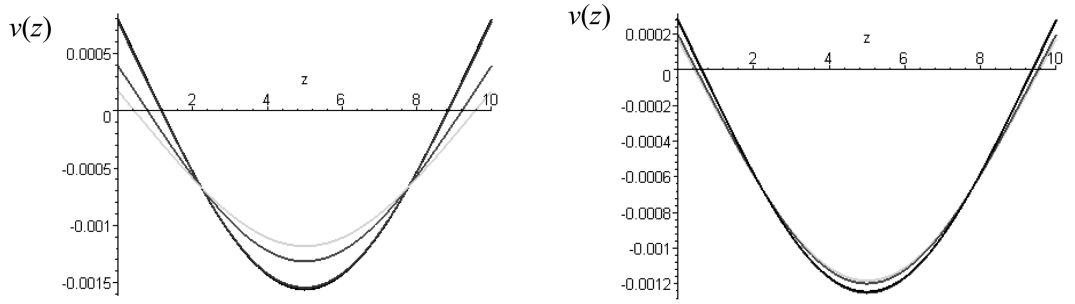

Fig. 15 Free end beam, creep aging model: time evolution of the displacement (m) for loading in $t' = 100$ days (left), and in $t' = 1000$ days (right); green line $t = 0$ days after loading, brown 100 days after loading, blue 1000 days, black 10000 days

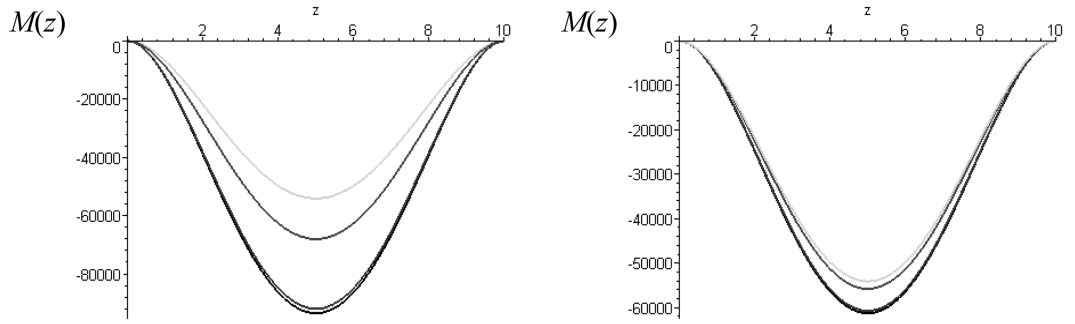

Fig. 16 Free end beam, creep aging model: time evolution of the bending moment (N·m) for loading in $t' = 100$ days (left), and in $t' = 1000$ days (right); green line $t = 0$ days after loading, brown 100 days after loading, blue 1000 days, black 10000 days

instant. The variation in time of the shear force (bottom plot of Fig. 13) is quite similar to that of the bending moment. The shear force diagrams too are regular. Note that at 1000 days after the loading the final values of all the quantities are nearly reached.

The same analysis has been performed adopting the aging creep model. For $t_0 = 0$ the results deriving from the aging model are similar to those of the hereditary model, and they are not shown. The final values of the three quantities under consideration are a few larger, even if the loading time is the same.

In order to highlight the differences in the responses for loading times $t' > t_0 = 0$, the analyses have been repeated for $t' = 100$, 1000 days using the aging model. In Figs. 15, 16 there are the plots of the displacements and of the bending moment, respectively. When the beam is loaded in $t' = 100$ days, viscous strains still develop, so that both the diplacements and the bending moment increase, more markedly the latter. For loading in $t' = 1000$ days the viscous strains are small; after loading the deflected line varies negligibly. On the other hand, the bending moment is still affected by the creep, and it has a 15% about increase. Similar comments can be made regarding the evolution in time of the shear force that is not reported for brevity's sake.

It is evident that the specific features of the diagrams of both the kinematic and static quantities of a beam depend on the load and the restraints. Thus, not all that has been shown here can be generalized. On the other hand, some general conclusions can be drawn. If a concrete beam is

loaded in early ages from hardening, there are more viscous deformations, and the hereditary and aging models for creep are both appropriate, even if the former is perhaps preferable. As the loading time is delayed, the viscous effects are lesser, what cannot be seized by the hereditary creep model. Thus, the use of the aging model for creep is compulsory. Moreover, as is can be noted in the previous plots, the final deflections and internal forces are smaller if the load is applied later.

5.3 Hinged-hinged beam with concentrated load

Now, let us consider a hinged-hinged beam with a concentrated force P in its midspan. In order to analyze this case, the concentrated force is expanded in a sine series according to Eqs. (50), (51), in which the first 35 odd terms are retained. Since the load is constant in time, the viscous modes are given by Eq. (37). In Eq. (15), which expresses the deflection, there are only the odd terms: in fact, in the expression (20) of the modal loads the integral in the numerator is zero when the eigenfunction $\phi_k(z)$ is even, while it alternately takes the values $L/2$, $-L/2$ times the constant $2P/LEI_{yy}$ for every odd eigenfunction. The denominator of Eq. (20) is always worth $L/2$ so that the odd modal loads are

$$Q_1 = \frac{2P}{LEI_{yy}}, \quad Q_3 = -\frac{2P}{LEI_{yy}}, \quad Q_5 = \frac{2P}{LEI_{yy}}, \quad Q_7 = -\frac{2P}{LEI_{yy}} \ \ldots \tag{55}$$

The eigenvalues, $k\pi/L$, the coupling paremeters D_k, and the coefficient γ_k/D_k, which is worth 19.9553 for any mode, are the same as those of the beam with uniformly distributed load. The

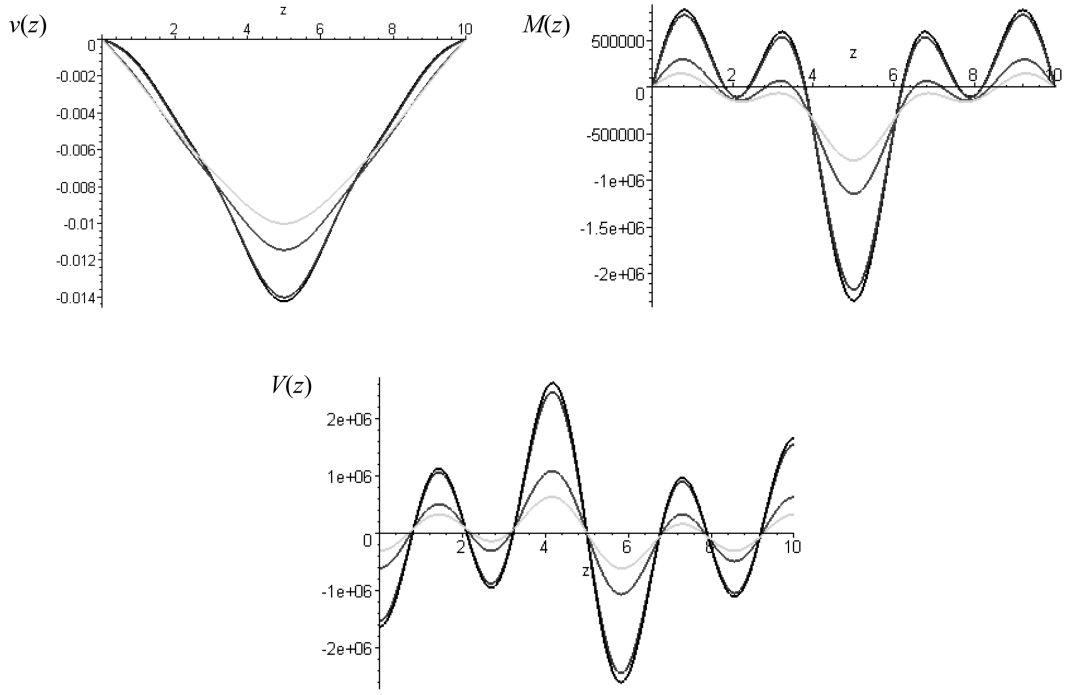

Fig. 17 Hinged-hinged beam with concentrated load P: viscoelastic diagrams of the displacements (top left) (m), of the bending moment (top right) (N·m), and of the shear force (bottom) (N) with the aging model; t = 0 days green, t = 100 days brown, t = 1000 days blue, t = 10000 days black

computations are performed for P = 1000 kN, while the other parameters are those of the previous examples. The rheological model is the aging one.

The diagrams of the displacement and of the internal forces are in Fig. 17, where the signs are opposite to the usual conventions for these quantities because of the computer program used to draw them. One can note: (1) the viscous deformations cause marked increases of all the quantities; (2) at 10000 days after loading the deflection increase is a 50%, the bending moment almost quadruples, while the shear force increase is even larger; (3) the first viscous mode is dominant on the deflected line, while other two modes are important for both the bending moment and shear force; (4) the actual load is a concentrated force, which is replaced by a truncated Fourier series, which is a continuous functions so that the cusp of the bending moment and the jump of the shear force are absent. Nevertheless, the bending moment diagram is not much far from the actual one. On the contrary, in order to reproduce the jump, the series (50) should retain much more than the 35 terms that have been used, which would make the computations more involved. However, the shear values are acceptably matched.

6. Conclusions

This paper is aimed at studying the interaction between a viscoelastic beam and an elastic medium. Such a type of coupled problem is found in analyzing the foundation beams. The equations that govern the problem are established basing the analysis on the assumption that the beam and the medium have a bilateral contact. This assumption is the first requirement to obtain an analytic solution. This type of solution is pursued as it is considered more suitable even for the engineering purpose.

From a theoretical point of view the medium that the beam is resting on may have any constitutive law. However, out of the elastic models an analytic solution is hardly conceivable. The most relevant elastic models that have been used to idealize a soil are due to Boussinesq and to Winkler, respectively. Boussinesq's model idealizes a soil as a homogeneous isotropic linearly elastic half space: in this way, a force acting in a point on the boundary of the half space causes effects - stresses, strain, displacements - to the infinity. Viceversa, Winkler's model is a local one: the medium becomes an ensemble of elastic springs, ideally being a spring present in any point of the boundary; the springs are independent so that there is no transmission of shear, and the effects of a force are localized in the point where this acts. Clearly, in any contact point the respect of the displacement compatibility is required.

The equilibrium equation of the beam is obtained by combining plane section law with the uniaxial viscous stress-strain relationship: it results as an integro-differential equation. In the case of an elastic medium, the compatibility may be expressed in integral form (Eq. (10)) by means of specific Green functions. Thus, the problem is governed by an integro-differential and an integral equation.

The Green's function of a Winkler's medium is a Dirac delta so that the integral expressing the compatibility becomes an algebraic expression, which is easily substituted in the beam equilibrium equation. An analytical solution having the form of an infinite series is found for both the cases of beam with restrained ends and of free-end beam. The deflection along the beam axis is given by the eigen-functions of the free vibrations of the same beam, while the variation in time is led by the so called reduced relaxation function. This function is associated with the varied creep kernel, that is

the ordinary creep kernel multiplied by a parameter D_k, which measures the relative compliance between the beam and the elastic medium in the k-th term of the series. The reduced relaxation function exists in analytical form for both hereditary and aging viscous models, while it results in numerical form for the creep kernels given by the product of a hereditary function times an aging one. In any case, the reduced relaxation function decreases with time so that the response increases.

The applications regard a concrete beam resting on a Winkler's soil. The restrained beam is hinged-hinged at the boundaries. Otherwise, the beam has free ends. Either hereditary and aging viscous models have been used in the analyses.

When the load is applied in early ages, it is found that creep causes the displacements and the internal forces to increase notably in time, which is very important from an engineering point of view. As the loading time is delayed, the viscous effects become lesser and lesser. The hereditary model cannot seize this behavior since the material properties are constant in time in this model. Thus, if the load is applied in advanced times, the use of the aging creep model is compulsory. However, by assuming the elastic modulus constant in time as it is customarily made, the computations are not more involved with respect to those of the hereditary model. In both cases, all formulae are analytic, and can be easily evaluated on a personal computer. The computations are longer and more involved only in the case of concentrated or partially distributed loads, particularly when the beam has free ends because such loads must be expanded in Fourier series, many terms of which are to be retained.

References

American Concrete Institute - ACI (1992), "Prediction of creep, shrinkage and temperature effects in concrete structures", Report no. 209R-92, Detroit (MI).

Aroutiounian, N.K. (1957), *Application de la Théorie du Fluage*, Eyrolles, Paris, France. (in French)

Avramidis, I.E. and Morfidis, K. (2006), "Bending of beams on three-parameters elastic foundation", *Int. J. Solids Struct.*, **43**, 357-375.

Bažant, Z.P. (1972), "Prediction of concrete creep using age-adjusted-effective-modulus-method", *ACI J.*, **69**(4).

Bažant, Z.P. (1988), *Mathematical Modeling of Creep and Shrinkage of Concrete*, John Wiley & Sons, New York.

Bažant, Z.P. and Chern, J.C. (1985), "Triple power law for concrete creep", *J. Eng. Mech.*, **111**(1), 63-83.

Bažant, Z.P. and Panula, L. (1978), "Basic creep", *Mater. Struct.*, **85**(11), 317-328.

Boussinesq, J. (1878), "Équilibre d'élasticité d'un sol isotrope sans pésanteur supportant différents poids", *Comptes Rendus*, **86**, 1260-1263. (in French)

Bowles, J.E. (1982), *Foundation Analysis and Design*, 3rd edition, Mc-Graw Hill, New York.

CEB-Comité Eurointernational du Béton (1984), *CEB Design Manual on Structural Effects of Time Dependent Behavior of Concrete*. CEB Bull. n. 142, Georgi Publishing Co., Saint Saphorin, Switzerland.

CEB-Comité Eurointernational du Béton (1993), *CEB-FIP Model Code 1990*. CEB Bull. n, 213/214, Thomas Telford, London (UK).

Clough, R.W. and Penzien, J. (1982) *Dynamics of Structures*, 3rd edition, Mc Graw Hill, New York.

Creus, G.J. (1985), *Viscoelasticity - Basic Theory and Applications to Concrete Structures*, Lectures Notes in Engineering 16, Springer Verlag, Berlin, Germany.

Elfesoufy, Z. and Azrar, L. (2005), "Buckling, flutter and vibration analyses of beams by integral equation formulations", *Comput. Struct.*, **83**, 2632-2649.

Flamant, A. (1892), "Sur la répartition des pressions dans un solide rectangulaire chargé transversale-ment", *Comptes Rendus*, **114**, 1465-1468. (in French)

Freudenthal, A.M. and Lorsh, H.G. (1957), "The infinite elastic beam on a linear viscoelastic foundation", *J.*

Eng. Mech. Div., **83**(1), 1158.
Gorman, D.J. (2008), "On use of the Dirac delta function in the vibration analysis of elastic structures", *Int. J. Solids Struct.*, **45**, 4605-4614.
Kargarnovin, M.H., Younesian, D., Thompson, D.J. and Jonesc, J.C. (2005), "Response of beams on nonlinear viscoelastic foundations to harmonic moving loads", *Comput. Struct.*, **83**, 1865-1877.
Kerr, A.D. (1964), "Elastic and viscoelastic foundation models", *J. Appl. Mech.*, **31**, 491-498.
Kerr, A.D. (1985), "On the determination of foundation model parameters", *J. Geotech. Eng.*, **111**(11), 1334-1340.
Kim, S.M. and Cho, Y.H. (2006), "Vibration and dynamic buckling of shear beam-columns on elastic foundation under moving harmonic loads", *Int. J. Solids Struct.*, **43**, 393-412.
Kuczma, M.S. and Demkowicz, L. (1992), "An adaptive algorithm for unilateral viscoelastic contact problems for beams and plates", *Comp. Meth. Appl.Mech. Eng.*, **101**, 183-196.
Kuczma, M.S. and Świtka, R. (1990), "Bending of elastic beams on Winkler-type viscoelastic foundation with unilateral constraints", *Comput. Struct.*, **34**(1), 125-136.
Lancioni, G. and Lenci, S. (2010), "Dynamics of a semi-infinite beam on unilateral springs: Touch-down points motion and detached bubbles propagation", *Int. J. Nonlin. Mech.*, **45**, 876-887.
Lee, E.H. and Radok, I.R. (1960), "The contact problem for viscoelastic bodies", *J. Appl. Mech.*, **27**, 438-444.
Mola, F. (1982), "Applicazioni del metodo delle funzioni di rilassamento ridotte all'analisi di strutture viscoelastiche non omogenee", *Studi e Ricerche n. 4*, Corso di Perfezionamento per le Costruzioni in Cemento Armato Fratelli Pesenti, Tamburini, Milano, 211-235. (in Italian)
Morfidis, K. (2010), "Vibration of Timoshenko beams on three-parameter elastic foundation", *Comput. Struct.*, **88**, 294-308.
Morfidis, K. and Avramidis, I.E. (2002), "Formulation of a generalized beam element on a two-parameter elastic foundation with semi-rigid connections and rigid offsets", *Comput. Struct.*, **80**, 1919-1934.
Muscolino, G. and Palmeri, A. (2007), "Response of beams resting on viscoelastically damped foundation to moving oscillators", *Int. J. Solids Struct.*, **44**, 1317-1336.
Nobili, A. and Tarantino, A.M. (2005), "Unilateral contact problem for aging viscoelastic beams", *J. Eng. Mech.*, **131**(12), 1229-1238.
Nowacki, W. (1970), *Théorie du Fluage*, Eyrolles, Paris, France. (in French)
Pasternak, P.L. (1954), "On a new method of analysis of an elastic foundation by means of two foundation constants", *Gosudarstvennoe Izdatelstro Liberaturi po Stroitelstvui Arkhitekture*, Moscow. (in Russian)
Pister, K.S. and Williams, M.L. (1960), "Bending of plates on a viscoelastic foundation", *J. Eng. Mech. Div.*, **86**, 31-44.
Raymondi, C. (1959), *Atti dell'Istituto di Scienza delle Costruzioni dell'Università di Pisa*, Vol. III n. 57, n. 60, n. 65. (in Italian)
Reissner, E. (1958), "Deflection of plates on viscoelastic foundation", *J. Appl. Mech.*, **25**, 144-145.
Sun, L. (2001), "A closed-form solution of a Bernoulli-Euler beam on a viscoelastic foundation under harmonic line loads", *J. Sound Vib.*, **242**(4), 619-627.
Sun, L. (2007), "Steady-state dynamic response of a Kirchhoff's slab on viscoelastic foundation to moving harmonic loads", *J. Appl. Mech.*, **74**, 1212-1224.
Timoshenko, S.P. and Goodier, J.N. (1970), *Theory of Elasticity*, Mc Graw Hill, New York.
Winkler, E. (1867), *Die Lehre von der Elasticität und Festigkeit*, Dominicus, Prague, Czech Rep. (in German)

Appendix - Recalls on the viscosity

For the reader's convenience, the fundamental principles of the linear viscosity are recalled. Papers and books on the viscoelasticity are very numerous: reference can be made to Aroutiounian (1957), Nowacki (1970), Creus (1985), Bažant (1988).

As an isotropic elastic continuum is characterized by two constants, the Young's modulus E and the Poisson ratio ν or the Lamé's constants λ and μ, an isotropic viscoelastic continuum is characterized by two functions, which are the volumetric $J_V(t, t')$ and the deviatoric $J_D(t, t')$ creep functions. In engineering notation, these functions can be replaced by the uniaxial creep function $J(t, t')$ and the viscous Poisson ratio $\nu(t, t')$. Clearly, in the case of a homogeneous and isotropic beam, these two functions are required even though the plane section law is assumed, and the shear deformability is disregarded. However, for many materials exhibiting creep the Poisson ratio can be considered independent of time as will be assumed here. For concrete this statement holds true if the water content has negligible changes in time (Bažant 1988). Under this assumption, the viscous properties are fully characterized either by the creep (compliance) function $J(t, t')$ or by the relaxation function $R(t, t')$, where:

- $J(t, t')$ represents the strain per unit stress, i.e., the response at time t to a sustained constant unit imposed stress applied at time t';
- $R(t, t')$ is the stress response at time t to a sustained constant unit imposed strain applied at time t'.

Hence, the stress-strain relationships for constant stress or strain are written as

$$\varepsilon(t, t') = \sigma_0 J(t, t') \qquad \sigma(t, t') = \varepsilon_0 R(t, t') \tag{56, 57}$$

The functions $J(t, t')$ and $R(t, t')$ are not independent: were they independent, the hypothesis of viscous properties described by only a function would be contradicted. They are related by a Volterra integral equation that can be expressed in the following equivalent forms

$$1 = R(t_0, t_0)J(t, t_0) + \int_{t_0}^{t} J(t, t')\frac{\partial R(t', t_0)}{\partial t'}dt' = E_c(t_0)J(t, t_0) + \int_{t_0}^{t} J(t, t')\frac{\partial R(t', t_0)}{\partial t'}dt' \tag{58}$$

$$1 = J(t, t_0)\cdot E_c(t_0) + \int_{t_0}^{t} J(t, t')\frac{\partial R(t', t_0)}{\partial t'}dt' \qquad 1 = \frac{R(t, t_0)}{E_c(t_0)} + \int_{t_0}^{t} R(t, t')\frac{\partial J(t', t_0)}{\partial t'}dt' \tag{59, 60}$$

If the applied stress or strain is variable in time, in the linear theory of viscoelasticity the superposition principle in time is postulated. Thus, the strain or the stress at time t for loading starting in t_0 are, respectively

$$\varepsilon(t, t_0) = \varepsilon_n(t) + \sigma(t_0)J(t, t_0) + \int_{t_0}^{t} J(t, t')\frac{d\sigma(t')}{dt'}dt' \tag{61}$$

$$\sigma(t, t_0) = [\varepsilon(t_0) - \varepsilon_n(t_0)]R(t, t_0) + \int_{t_0}^{t} R(t, t')\frac{d[\varepsilon(t') - \varepsilon_n(t')]}{dt'} \tag{62}$$

where $\varepsilon_n(t)$ is a stress-independent inelastic strain such as shrinkage or thermal strain; $\sigma(t_0)$ and $\varepsilon(t_0)$ are the initial values for $t' = t_0$ of the stress or the strain, respectively.

As a principle, the function J (or R) should be established on the basis of experimental measurements preserving some thermodynamical requirements. However, these models have some shortcomings, and in engineering practice is often customary to use two theoretical models, the hereditary model (Kelvin-Voigt) and the aging model (Krall-Dishinger-Whitney).

In the hereditary model the elastic and rheological properties of a material do not vary in time so that the elapsed time $(t - t')$ only determined the response. The principal functions of this model are

$$J(t, t_0) = \frac{1}{E}\{1 + \varphi_\infty[1 - \exp[-\alpha(t - t_0)]]\} \tag{63}$$

$$L(t, t') = -E\frac{\partial J(t, t')}{\partial t'} = \alpha\varphi_\infty \cdot \exp[-\alpha(t - t')] \tag{64}$$

$$R(t, t_0) = \frac{E}{1+\varphi_\infty}\{1 + \varphi_\infty \cdot \exp[-\alpha(1+\varphi_\infty)(t-t_0)]\} \tag{65}$$

In previous equations a measures the creep velocity (s^{-1} or $days^{-1}$), while φ_∞ is ratio between the final viscous strain ($t = \infty$) and the initial elastic strain $[\varepsilon_e(t_0) = \sigma(t_0)/E]$. $L(t, t')$ is defined as the viscous kernel.

Analogously, a relaxation kernel is given by $K(t, t') = -\frac{1}{E}\frac{\partial R(t, t')}{\partial t'}$.

In Fig. 18 the two fundamental features of the hereditary model are shown: (1) the creep curves are parallel in horizontal; (2) if a stress σ_0 is applied in t_0 and removed in t, in this instant the elastic strain σ_0/E is recovered, then the creep strains developed between t_0 and t are gradually recovered, and for $t = \infty$ the material is unstrained (due to the exponential behavior of the functions (66)-(68) zero strain is practically reached in a finite time).

In the classic aging model it is assumed that the curves giving the viscous strains for different loading instants $t_0 < t_1 < \ldots < t_k$ are parallel in vertical (Fig. 19, left), that is

$$C(t, t_1) = C(t, t_0) - C(t_1, t_0) \tag{66}$$

where the function $C(t, t_1)$ gives the viscous strain for unit applied stress. As a consequence of this hypothesis the kernels depend on t' only and not on t, while t_0 becomes a parameter, the first instant in which the material can be loaded.

The principal function of the classic aging model are

$$J(t, t') = \frac{1}{E(t')} + C(t, t') = \frac{1}{E(t')} + \frac{\varphi_\infty}{E_0}\{\exp[-\beta(t'-t_0)] - \exp[-\beta(t-t_0)]\} \tag{67}$$

$$L(t, t') = \beta\varphi_\infty \cdot \exp[-\beta(t'-t_0)] = L(t') \tag{68}$$

$$R(t, t') = E \cdot e^{-\varphi_\infty\{\exp[-\beta(t'-t_0)] - \exp[-\beta(t-t_0)]\}} \tag{69}$$

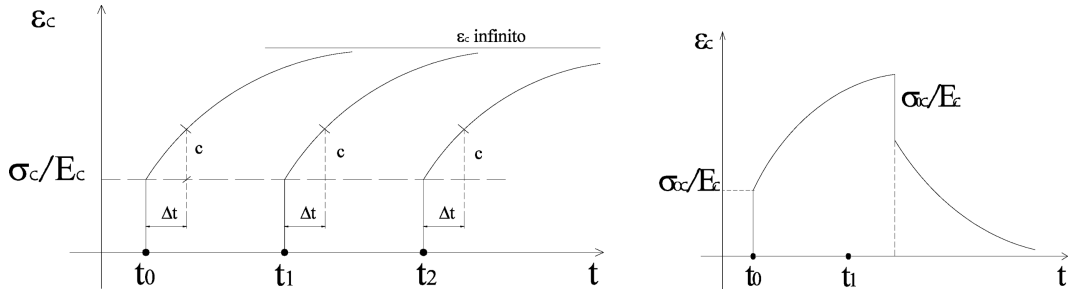

Fig. 18 Loading curve (left) and loading-unloading curve (right) of the hereditary model (left)

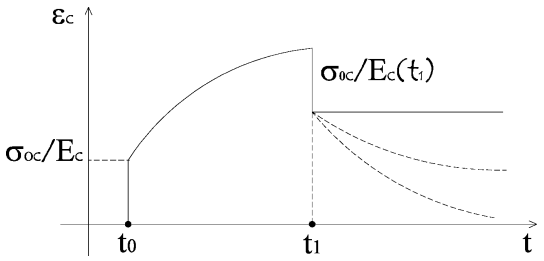

Fig. 19 Loading (left) and loading-unloading (right) curves for the aging viscous model

In Eq. (67) E_0 is a reference value of the elastic modulus. Very often in the applications the variability in time is disregarded, and a constant value E of the elastic modulus is used as in Eqs. (68), (69). If the material is loaded in t_0, the changes in Eqs. (67)-(69) are straightforward.

In the right plot of Fig. 19 a fundamental feature of the aging model is depicted: if an aging visco-elastic material is subjected to a loading path with the application of σ_0 in t_0 and the removal of it in t_1, in this instant the elastic strain $\sigma_0/E(t_1)$ is recovered. Since the creep curves are parallel in vertical, after t_1 the strain remain constant, which means that the aging viscous model is viscoplastic.

On the other hand, the real materials show neither a purely hereditary behavior or a purely aging one, but they behave in an intermediate fashion. Thus, after removing the stress qualitatively the strain changes like in the dashed curves of Fig. 19 (right). In order to seize the actual behavior of the materials, since many years the so-called viscous product models were proposed (Aroutiounian 1957, Bažant and Panula 1978, Bažant and Chern 1985, American Concrete Institute 1992, CEB 1984, 1993). They have the form

$$J(t, t') = \frac{1}{E(t')} + \frac{1}{E(t')} J_h(t - t') \cdot J_a(t') \tag{70}$$

in which J_h is a hereditary function and J_a an aging one. Unfortunately, none of the product models leads to an analytical solution of the integral Eqs. (58)-(60), which results in numeric relaxation functions. A numeric $R(t, t')$ is not suitable for engineering computation: thus, the classic hereditary and aging models are still in use, and in the final step of the present theoretical study reference is made to them.